# Effective Properties of Multi-layered Multi-functional Composites

**Byeong-Chan Kim** [a], **Arturo Baltazar** [b] **and Jin-Yeon Kim** [c,*]

[a] Department of Civil Engineering, Hanbat University, SAN 16-1 Duckmyoung-Dong, Yusung-Gu, Daejeon 305-719, Korea
[b] Programa de Robótica y Manufactura Avanzada, CINVESTAV, Carretera Saltillo-Monterrey Km 13.5, Ramos Arizpe, Coah, 25900 México
[c] School of Civil and Environmental Engineering, Georgia Institute of Technology, 790 Atlantic Drive, Atlanta, GA 30332, USA

**Abstract**
A matrix method for evaluating effective electro-magneto-thermo-elastic properties of a generally anisotropic multilayered composite is presented. Physical variables are categorized into two groups: one that satisfies the continuity across the interface between layers and another that satisfies an average inter-layer compatibility (which is also exact). The coupled electro-magneto-thermo-elastic constitutive equation is accordingly reassembled into submatrices, which leads to the derivation of concise and exact matrix expressions for effective properties of a multilayered composite having the coupled physical effects. Comparing the results for a purely elastic multiplayer with those from other theoretical approaches validates the developed method. Examples are given for a PZT-graphite/epoxy composite and a BaTiO$_3$–CoFe$_2$O$_4$ multilayer which exhibit piezo-thermoelastic and magnetoelectric properties, respectively. The result shows how a strong magnetoelectric effect can be achieved by combining piezoelectric and piezomagnetic materials in a multilayered structure. The magnetoelectric coefficient of the BaTiO$_3$–CoFe$_2$O$_4$ multilayer is compared with those for fibrous and particulate composites fabricated with the same constituents.
© Koninklijke Brill NV, Leiden, 2009

## 1. Introduction

In recent years, the multilayered composites with piezoelectric, thermoelectric and magnetoelectric effects have found an increasing number of applications in sensor/actuator technology, smart materials and microelectronics. The simultaneous

---

\* To whom correspondence should be addressed. E-mail: jykim@gatech.edu
Edited by KSCM

magnetoelectric effect that is rarely found in monolithic materials (e.g., [1]) can be easily achieved by constructing a two-phase composite [2] (in a multilayer or inclusion-matrix type composite) with components having piezoelectric and piezomagnetic effects. These multilayers may be formed as a several hundred-micron-thick layer, e.g., the thin film on infrared detectors, or as a large-scale structure, e.g., the smart composite patch for controlling aircraft-wing flutter. These active properties of materials are often incorporated into the conventional composites to meet the practical requirements of high stiffness and strength, low thermal expansion, high thermal conductivity, etc. For the design and analysis of such composites for applications to smart structures, the capability of predicting effective (overall) material properties and especially whether the desired cross-properties are achieved, is essentially required. To analyze the effective material properties of the new multi-functional composites with combined piezoelectric, piezomagnetic, thermoelectric and thermomagnetic effects, one needs a general approach that can deal with these different physical effects in a unified way.

The determination of the effective material properties of layered media has long been an interest in many different areas, including geophysics and micromechanics. The effective elastic and thermoelastic properties of layered composites have been analyzed by many authors [3–6]. Akcakaya and Farnell [7] investigated on the effective elastic and piezoelectric constants of superlattices. Recently, Chen *et al.* [8] employed the Mori–Tanaka's self-consistent mean field approximation scheme in conjunction with the continuity conditions at layer interfaces to obtain the effective properties of multilayer composites. In general, it should be noted that the layered medium is one of few composite types for which *exact* effective material properties can be obtained for its simple geometry [3]. Therefore, unlike with the inclusion-matrix type composites, an approximate averaging scheme is not necessary in the analysis of the effective properties of layered composites.

In this paper, our previous work [6] on the purely elastic multilayers is extended and generalized to multilayers with various physical effects. Examples of calculating effective properties of a piezo-thermoelastic (PZT-graphite/epoxy) and piezoelectric–piezomagnetic ($BaTiO_3$–$CoFe_2O_4$) composites are given. The effective electric, magnetic, thermal and elastic properties are presented for varying volume fraction of a constituting layer. Especially for the $BaTiO_3$–$CoFe_2O_4$ composite, the magnetoelectric coefficient is compared with those of fiber–matrix and particulate composites to validate the present approach and the calculated results.

## 2. Effective Properties of Electro-Magneto-Thermo-Elastic Multilayer Composites

### 2.1. Constitutive Equations

The constitutive equations for an anisotropic thermoelastic solid having piezoelectric, piezomagnetic, thermoelectric and thermomagnetic effects are given by:

$$\boldsymbol{\sigma} = \mathbf{C}\boldsymbol{\varepsilon} - \mathbf{e}^{\mathrm{T}}\mathbf{E} - \mathbf{q}^{\mathrm{T}}\mathbf{H} - \boldsymbol{\gamma}\Delta\theta, \tag{1}$$

$$\mathbf{D} = \mathbf{e}\boldsymbol{\varepsilon} + \boldsymbol{\kappa}\mathbf{E} + \boldsymbol{\zeta}\mathbf{H} + \mathbf{p}\Delta\theta, \tag{2}$$

$$\mathbf{B} = \mathbf{q}\boldsymbol{\varepsilon} + \boldsymbol{\zeta}^{\mathrm{T}}\mathbf{E} + \boldsymbol{\lambda}\mathbf{H} + \mathbf{m}\Delta\theta, \tag{3}$$

$$s = \boldsymbol{\gamma} \cdot \boldsymbol{\varepsilon} + \mathbf{p}\mathbf{E} + \mathbf{m}\mathbf{H} + c_v\Delta\theta, \tag{4}$$

where $\boldsymbol{\sigma}$ and $\boldsymbol{\varepsilon}$ are the stress and strain; $\mathbf{C}$ is the elastic stiffness; $\mathbf{E}$ and $\mathbf{D}$ are the electric field and the electric displacement; $\mathbf{e}$ and $\boldsymbol{\kappa}$ are the piezoelectric coefficient and the dielectric constant; $\mathbf{H}$ and $\mathbf{B}$ are the magnetic field and the magnetic induction; $\mathbf{q}$ and $\boldsymbol{\lambda}$ are the piezomagnetic coefficient and the magnetic permeability; $\boldsymbol{\zeta}$ is the magnetoelectric coefficient; $s$ and $\Delta\theta$ are the entropy per unit volume and the temperature change from the ambient temperature ($\theta_0$); the heat capacity per unit volume at a constant strain is $c_v\theta_0$ and the thermal stress coefficient $\boldsymbol{\gamma}$ is related with the thermal expansion coefficient $\boldsymbol{\beta}$ by $\boldsymbol{\gamma} = \mathbf{C}\boldsymbol{\beta}$; $\mathbf{p}$ and $\mathbf{m}$ are the thermoelectric and thermomagnetic coefficients. In this derivation, all coefficient matrices are assumed as full-matrix allowing the general anisotropy in the material properties.

Constitutive equations for a material lacking some of the physical effects can be readily obtained from (1)–(4). For example, those for a composite with piezoelectric and piezomagnetic effects are:

$$\boldsymbol{\sigma} = \mathbf{C}\boldsymbol{\varepsilon} - \mathbf{e}^{\mathrm{T}}\mathbf{E} - \mathbf{q}^{\mathrm{T}}\mathbf{H}, \tag{5}$$

$$\mathbf{D} = \mathbf{e}\boldsymbol{\varepsilon} + \boldsymbol{\kappa}\mathbf{E} + \boldsymbol{\zeta}\mathbf{H}, \tag{6}$$

$$\mathbf{B} = \mathbf{q}\boldsymbol{\varepsilon} + \boldsymbol{\zeta}^{\mathrm{T}}\mathbf{E} + \boldsymbol{\lambda}\mathbf{H}. \tag{7}$$

Likewise, those for a piezo-thermoelastic composite are:

$$\boldsymbol{\sigma} = \mathbf{C}\boldsymbol{\varepsilon} - \mathbf{e}^{\mathrm{T}}\mathbf{E} - \boldsymbol{\gamma}\Delta\theta, \tag{8}$$

$$\mathbf{D} = \mathbf{e}\boldsymbol{\varepsilon} + \boldsymbol{\kappa}\mathbf{E} + \mathbf{p}\Delta\theta, \tag{9}$$

$$s = \boldsymbol{\gamma} \cdot \boldsymbol{\varepsilon} + \mathbf{p}\mathbf{E} + c_v\Delta\tilde{\theta}. \tag{10}$$

## 2.2. Compatibility Conditions

Consider an infinite multilayer that is constructed by periodically stacked up a unit cell of an arbitrary number of layers. The unit cell consisting of $N$ layers taken from the periodic medium shown in Fig. 1 is considered as a representative volume element (RVE). The REV is assumed to have layers with thicknesses $h_1, h_2, \ldots, h_N$ in $x_2$ direction. The perfect rigid contact at all interfaces between layers is assumed.

To analyze the effective material constants, the average responses of the RVE to a uniform in-plane or out-of-plane mechanical load (or other field applications) are considered. As in the purely elastic multilayers [6], it is established that the average of any physical variable should satisfy one of the two compatibility conditions. The first condition is the continuity across the interfaces. When a physical variable ($f$) is continuous across the interfaces, the average of the variable is automatically equal to those of individual layers:

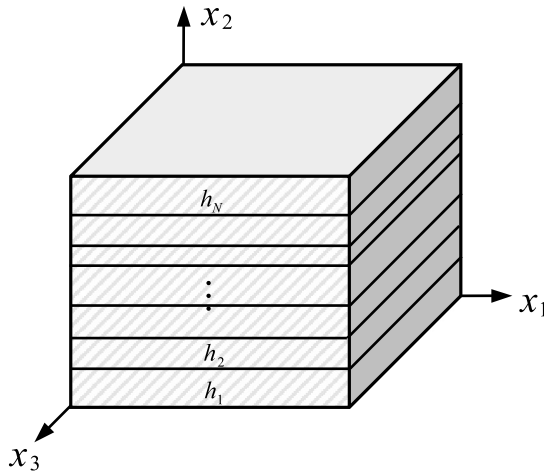$$\bar{f} = f^{(1)} = f^{(2)} = \cdots = f^{(N)}. \tag{11}$$

**Figure 1.** Representative volume element of a periodic multilayer.

The overbar denotes the average of a physical quantity (e.g., the stress) and the effective value of a material constant. The second condition is that the average of a certain physical quantity is determined as the volume-fraction weighted average of those in all layers:

$$\bar{g} = g^{(1)}v_1 + g^{(2)}v_2 + \cdots + g^{(N)}v_N, \tag{12}$$

where $v_i \ (= h_i/h)$ is the volume fraction of the $i$th layer and $h = (h_1 + h_2 + \cdots + h_N)$. For example, the average out-of-plane electric displacement $(\bar{D}_2)$ is equal to that in one of the layers since the out-of-plane electric displacement should be continuous across all interfaces, whereas the average in-plane electric displacements $(\bar{D}_1, \bar{D}_3)$ are the volume fraction weighted average of those in layers. In this way, it is found that in-plane strain, in-plane electric and magnetic fields, out-of-plane stress, out-of-plane electric displacement, out-of-plane magnetic induction and the temperature deviation should satisfy the continuity compatibility, equation (11). It is also found that out-of-plane strain, out-of-plane electric and magnetic fields, in-plane stress, in-plane electric displacement, in-plane magnetic induction and the entropy should satisfy the second compatibility, equation (12).

To apply the matrix formulation that has been developed for effective elastic constants [6], the above constitutive equations for the $i$th layer are reassembled such that physical variables which satisfy the two different compatibility conditions ((11) and (12)) are grouped in respective submatrices:

$$\left\{ \begin{array}{c} \boldsymbol{\tau}_\parallel^{(i)} \\ \boldsymbol{\tau}_\perp^{(i)} \end{array} \right\} = \left[ \begin{array}{cc} \mathbf{D}_\parallel^{(i)} & \mathbf{D}_\times^{(i)\mathrm{T}} \\ \mathbf{D}_\times^{(i)} & \mathbf{D}_\perp^{(i)} \end{array} \right] \left\{ \begin{array}{c} \boldsymbol{\eta}_\parallel^{(i)} \\ \boldsymbol{\eta}_\perp^{(i)} \end{array} \right\}, \tag{13}$$

where the submatrices $\mathbf{D}_\parallel^{(i)}, \mathbf{D}_\perp^{(i)}$ and $\mathbf{D}_\times^{(i)}$ are defined as material constants that relate the in-plane variables ($\boldsymbol{\tau}_\parallel^{(i)}$ to $\boldsymbol{\eta}_\parallel^{(i)}$), that relate the out-of-plane variables ($\boldsymbol{\tau}_\perp^{(i)}$

to $\eta_\perp^{(i)}$) and that cross-relate the in-plane and the out-of-plane variables ($\tau_\perp^{(i)}$ to $\eta_\parallel^{(i)}$ and $\tau_\parallel^{(i)}$ to $\eta_\perp^{(i)}$), respectively. Therefore, the field variable vectors in (13) satisfy the following conditions:

$$\bar{\eta}_\parallel = \eta_\parallel^{(1)} = \eta_\parallel^{(2)} = \cdots = \eta_\parallel^{(N)}, \tag{14}$$

$$\bar{\eta}_\perp = \eta_\perp^{(1)} v_1 + \eta_\perp^{(2)} v_2 + \cdots + \eta_\perp^{(N)} v_N, \tag{15}$$

$$\bar{\tau}_\parallel = \tau_\parallel^{(1)} v_1 + \tau_\parallel^{(2)} v_2 + \cdots + \tau_\parallel^{(N)} v_N, \tag{16}$$

$$\bar{\tau}_\perp = \tau_\perp^{(1)} = \tau_\perp^{(2)} = \cdots = \tau_\perp^{(N)}. \tag{17}$$

As an example, submatrices in the reassembled constitutive matrix for the piezoelectric–piezomagnetic material are presented in the followings. Representing the coupled constitutive equations in a matrix form, (5)–(7) can be written as:

$$\begin{Bmatrix} \sigma_{11} \\ \sigma_{22} \\ \sigma_{33} \\ \sigma_{23} \\ \sigma_{13} \\ \sigma_{12} \\ D_1 \\ D_2 \\ D_3 \\ B_1 \\ B_2 \\ B_3 \end{Bmatrix} = \begin{bmatrix} C_{11} & C_{12} & C_{13} & C_{14} & C_{15} & C_{16} & e_{11} & e_{21} & e_{31} & q_{11} & q_{21} & q_{31} \\ & C_{22} & C_{23} & C_{24} & C_{25} & C_{26} & e_{12} & e_{22} & e_{32} & q_{12} & q_{22} & q_{32} \\ & & C_{33} & C_{34} & C_{35} & C_{36} & e_{13} & e_{23} & e_{33} & q_{13} & q_{23} & q_{33} \\ & & & C_{44} & C_{45} & C_{46} & e_{14} & e_{24} & e_{34} & q_{14} & q_{24} & q_{34} \\ & & & & C_{55} & C_{56} & e_{15} & e_{25} & e_{35} & q_{15} & q_{25} & q_{35} \\ & & & & & C_{66} & e_{16} & e_{26} & e_{36} & q_{16} & q_{26} & q_{36} \\ & & & & & & -\kappa_{11} & -\kappa_{12} & -\kappa_{13} & -\zeta_{11} & -\zeta_{12} & -\zeta_{13} \\ & & SYM & & & & & -\kappa_{22} & -\kappa_{23} & -\zeta_{12} & -\zeta_{22} & -\zeta_{23} \\ & & & & & & & & -\kappa_{33} & -\zeta_{13} & -\zeta_{23} & -\zeta_{33} \\ & & & & & & & & & -\lambda_{11} & -\lambda_{12} & -\lambda_{13} \\ & & & & & & & & & & -\lambda_{22} & -\lambda_{23} \\ & & & & & & & & & & & -\lambda_{33} \end{bmatrix} \begin{Bmatrix} \varepsilon_{11} \\ \varepsilon_{22} \\ \varepsilon_{33} \\ \varepsilon_{23} \\ \varepsilon_{13} \\ \varepsilon_{12} \\ -E_1 \\ -E_2 \\ -E_3 \\ -H_1 \\ -H_2 \\ -H_3 \end{Bmatrix}. \tag{18}$$

Note that the constitutive matrix is written in a full-matrix form. The subvectors and submatrices in the reassembled constitutive matrix are:

$$\tau_\parallel = \{\sigma_{11}, \sigma_{33}, \sigma_{13}, D_1, D_3, B_1, B_3\}^{\mathrm{T}}, \tag{19}$$

$$\tau_\perp = \{\sigma_{22}, \sigma_{12}, \sigma_{23}, D_2, B_2\}^{\mathrm{T}}, \tag{20}$$

$$\eta_\parallel = \{\varepsilon_{11}, \varepsilon_{33}, \varepsilon_{13}, -E_1, -E_3, -H_1, -H_3\}^{\mathrm{T}}, \tag{21}$$

$$\eta_\perp = \{\varepsilon_{22}, \varepsilon_{12}, \varepsilon_{23}, -E_2, -H_2\}^{\mathrm{T}}, \tag{22}$$

$$\mathbf{D}_\parallel = \begin{bmatrix} C_{11} & C_{13} & C_{15} & e_{11} & e_{31} & q_{11} & q_{31} \\ & C_{33} & C_{35} & e_{13} & e_{33} & q_{13} & q_{33} \\ & & C_{55} & e_{15} & e_{35} & q_{15} & q_{35} \\ & & & -\kappa_{11} & -\kappa_{13} & -\zeta_{11} & -\zeta_{13} \\ & & SYM & & -\kappa_{33} & -\zeta_{13} & -\zeta_{33} \\ & & & & & -\lambda_{11} & -\lambda_{13} \\ & & & & & & -\lambda_{33} \end{bmatrix}, \tag{23}$$

$$\mathbf{D}_\perp = \begin{bmatrix} C_{22} & C_{24} & C_{26} & e_{22} & q_{22} \\ & C_{44} & C_{46} & e_{24} & q_{24} \\ & & C_{66} & e_{26} & q_{26} \\ & SYM & & -\kappa_{22} & -\zeta_{22} \\ & & & & -\lambda_{22} \end{bmatrix}, \tag{24}$$

$$\mathbf{D}_\times = \begin{bmatrix} C_{12} & C_{23} & C_{25} & e_{12} & e_{32} & q_{12} & q_{32} \\ C_{14} & C_{34} & C_{45} & e_{14} & e_{34} & q_{14} & q_{34} \\ C_{16} & C_{36} & C_{56} & e_{16} & e_{36} & q_{16} & q_{36} \\ e_{21} & e_{23} & e_{25} & -\kappa_{12} & -\kappa_{23} & -\zeta_{12} & -\zeta_{23} \\ q_{21} & q_{23} & q_{25} & -\zeta_{12} & -\zeta_{23} & -\lambda_{12} & -\lambda_{23} \end{bmatrix}. \tag{25}$$

### 2.3. Effective Material Properties

Now we proceed to derive the expressions for the effective material constants in terms of the material constants of the individual layers from the reassembled constitutive matrix (13) and the compatibility conditions (14)–(17). The constitutive relation for the effective medium can be expressed as:

$$\begin{Bmatrix} \bar{\tau}_\parallel \\ \bar{\tau}_\perp \end{Bmatrix} = \begin{bmatrix} \overline{\mathbf{D}}_\parallel & \overline{\mathbf{D}}_\times^{\mathrm{T}} \\ \overline{\mathbf{D}}_\times & \overline{\mathbf{D}}_\perp \end{bmatrix} \begin{Bmatrix} \bar{\eta}_\parallel \\ \bar{\eta}_\perp \end{Bmatrix}. \tag{26}$$

From (13) and (17), the following relation can be drawn:

$$\left[ \mathbf{D}_\times^{(i)} - \mathbf{D}_\times^{(j)} \right] \bar{\eta}_\parallel = -\mathbf{D}_\perp^{(i)} \eta_\perp^{(i)} + \mathbf{D}_\perp^{(j)} \eta_\perp^{(j)}. \tag{27}$$

Solving a system of linear equations consisting of (15) and (27), the vector $\eta_\perp^{(i)}$ in the $i$th layer is obtained as follows:

$$\eta_\perp^{(i)} = \mathbf{L}^{(i)} \bar{\eta}_\perp - \mathbf{L}^{(i)} \sum_{j=1}^{N} v_j \mathbf{D}_\perp^{(j)-1} \left[ \mathbf{D}_\times^{(i)} - \mathbf{D}_\times^{(j)} \right] \bar{\eta}_\parallel, \tag{28}$$

where

$$\mathbf{L}^{(i)} = \mathbf{D}_\perp^{(i)-1} \left[ \sum_{j=1}^{N} v_j \mathbf{D}_\perp^{(j)-1} \right]^{-1}. \tag{29}$$

From (13) and (14), one obtains:

$$\bar{\tau}_\perp = \mathbf{D}_\times^{(i)} \bar{\eta}_\parallel + \mathbf{D}_\perp^{(i)} \eta_\perp^{(i)}. \tag{30}$$

Substituting (28) into (30), one of the effective material constant submatrices is

$$\overline{\mathbf{D}}_\perp = \left( \sum_{i=1}^{N} v_i \mathbf{D}_\perp^{(i)-1} \right)^{-1}. \tag{31}$$

Similarly from (13), (14) and (16),

$$\bar{\tau}_\parallel = \sum_{i=1}^{N} v_i \mathbf{D}_\parallel^{(i)} \bar{\eta}_\parallel + \sum_{i=1}^{N} v_i \mathbf{D}_\times^{(i)\mathrm{T}} \eta_\perp^{(i)}. \tag{32}$$

Substituting (28) into (32), one can obtain the remaining submatrices:

$$\overline{\mathbf{D}}_\parallel = \sum_{i=1}^{N} v_i \left\{ \mathbf{D}_\parallel^{(i)} - \mathbf{D}_\times^{(i)\mathrm{T}} \mathbf{L}^{(i)} \sum_{j=1}^{N} v_j \mathbf{D}_\perp^{(i)-1} \left[ \mathbf{D}_\times^{(i)} - \mathbf{D}_\times^{(j)} \right] \right\}, \tag{33}$$

and

$$\overline{\mathbf{D}}_\times = \sum_{i=1}^{N} v_i \mathbf{D}_\times^{(i)} \mathbf{L}^{(i)\mathrm{T}}. \qquad (34)$$

Therefore, (31), (33) and (34) are the effective material constants of a generally anisotropic multilayer with coupled piezoelectric, piezomagnetic, thermoelectric and thermomagnetic effects. Explicit expressions for individual effective properties can be derived from these matrix equations but are not shown here due to the space limitation.

## 3. Examples

### 3.1. Elastic Multilayer Composites

To give a direct numerical validation of the present method, effective properties of a purely elastic multilayer, a graphite/epoxy [0/90] laminate composite, are compared with those calculated by two other approaches that have completely different theoretical foundations: the generalized method of cells (GMC) of Paley and Aboudi [9] and the dynamic homogenization theory (DHT) of Wang and Rokhlin [10]. The GMC is a semi-analytical technique that is capable of simulating mechanical behaviors of a composite material with an arbitrary microstructure. The DHT is a dynamical theory for predicting elastic wave propagation in a multiplayer composite. So, the effective static properties are obtained from the responses of the medium at a very low frequency. Elastic constants of the transversely isotropic graphite/epoxy lamina are presented in Table 1. As shown in Table 2, within the numerical tolerance, the results from the presented method are exactly coincident with those from the two different approaches, which proves that the present method and the calculated results are correct. Note that the effective medium exhibits a tetragonal symmetry that requires six independent elastic constants.

### 3.2. Piezo-thermoelastic Layers

A piezo-thermoelastic composite that is composed of orthotropic graphite/epoxy layers and transversely isotropic PZT layers is considered. The graphite/epoxy layer has a layup of $[0/90_3/\underline{0}]$s. The layer properties are presented also in Table 1. The overall properties of the graphite/epoxy layer are calculated from the lamina properties using (31), (33) and (34).

In Figs 2–6, the effective material properties of the PZT-graphite/epoxy composite are shown for varying volume fraction of the PZT layer. It is interesting to note that some material constants $(\overline{C}_{33}, \bar{\kappa}_1, \bar{\kappa}_3, \bar{e}_{21}, \bar{e}_{23}, \overline{P}_2)$ have an extremum at a certain intermediate volume fraction, which is useful in the material design [11]. It is also observed that only three constants $(\overline{C}_{55}, \overline{P}_1, \overline{P}_3)$ satisfy the rule of mixture (volume fraction-weighted average) while the others do not.

That an effective property has an extremum at an intermediate volume fraction is quite unexpected since the effective property is usually a monotonically increasing

**Table 1.**
Physical properties of constituents

Graphite/Epoxy Lamina
$C_{11} = 143.2$, $C_{12} = C_{13} = 7.5$, $C_{22} = C_{33} = 15.8$, $C_{23} = 8.2$, $C_{55} = 7.0$ (GPa)

Graphite/Epoxy $[0/90_3/0/90_3/0]$ Layer
$C_{11} = 54.0$, $C_{12} = 8.0$, $C_{13} = 7.5$, $C_{22} = 15.8$, $C_{23} = 7.5$, $C_{33} = 105.0$,
$C_{44} = 5.6$, $C_{55} = 7.0$, $C_{66} = 4.4$ (GPa)
$\kappa_{11} = \kappa_{22} = \kappa_{33} = 1.23 \times 10^{-8}$ (C$^2$/N m$^2$)
$\gamma_1 = 7.93 \times 10^6$, $\gamma_2 = 5.7 \times 10^6$, $\gamma_3 = 7.48 \times 10^6$ (N/K m$^2$)
$c_v = 4.11 \times 10^8$ (N/m$^2$ K$^2$)

PZT
$C_{11} = 120.3$, $C_{12} = 65.7$, $C_{13} = 75.2$, $C_{22} = 110.9$, $C_{44} = 21.9$ (GPa)
$e_{12} = e_{13} = 5.4$, $e_{22} = -15.1$, $e_{61} = -12.7$ (C/m$^2$)
$\kappa_{11} = 1.53 \times 10^{-8}$, $\kappa_{22} = 1.46 \times 10^{-8}$, $\kappa_{33} = 1.53 \times 10^{-8}$ (C$^2$/N m$^2$)
$\gamma_1 = 1.18 \times 10^6$, $\gamma_2 = 1.2 \times 10^6$, $\gamma_3 = 1.18 \times 10^6$ (N/K m$^2$)
$P_1 = 7.5 \times 10^{-4}$, $P_2 = -6.2 \times 10^{-4}$, $P_3 = 7.5 \times 10^{-4}$ (C/K m$^2$)
$c_v = 9.67 \times 10^8$ (N/m$^2$ K$^2$)

BaTiO$_3$
$C_{11} = 166.0$, $C_{12} = 77.0$, $C_{13} = 78.0$, $C_{33} = 162.0$, $C_{44} = 43.0$ (GPa)
$e_{31} = -4.4$, $e_{33} = 18.6$, $e_{34} = 11.6$ (C/m$^2$)
$\kappa_{11} = 1.12 \times 10^{-8}$, $\kappa_{33} = 1.26 \times 10^{-8}$ (C$^2$/N m$^2$)
$\lambda_{11} = 5.0 \times 10^{-6}$, $\lambda_{33} = 10.0 \times 10^{-6}$ (N s$^2$/C$^2$)

CoFe$_2$O$_4$
$C_{11} = 286.0$, $C_{12} = 173.0$, $C_{13} = 170.5$, $C_{33} = 269.5$, $C_{44} = 45.3$ (GPa)
$q_{31} = 580.3$, $q_{33} = 699.7$, $q_{34} = 550.0$ (N/A m)
$\kappa_{11} = 8.0 \times 10^{-11}$, $\kappa_{33} = 9.3 \times 10^{-11}$ (C$^2$/N m$^2$)
$\lambda_{11} = -5.9 \times 10^{-4}$, $\lambda_{33} = 1.57 \times 10^{-4}$ (N s$^2$/C$^2$)

**Table 2.**
Effective elastic constants calculated by the generalized method of cells (GMC), the dynamic homogenization theory (DHT) and the present method (unit: GPa)

|         | $C_{11}$ | $C_{33}$ | $C_{12}$ | $C_{23}$ | $C_{44}$ | $C_{66}$ |
|---------|----------|----------|----------|----------|----------|----------|
| GMC     | 79.429   | 15.800   | 7.508    | 7.850    | 4.926    | 7.000    |
| DHT     | 79.427   | 15.800   | 7.507    | 7.853    | 4.927    | 7.000    |
| Present | 79.428   | 15.801   | 7.508    | 7.851    | 4.927    | 7.000    |

or decreasing function. One possible cause of this behavior is the coupling between different physical effects. Let us examine this for $\overline{C}_{33}$ in Fig. 2. First, $\overline{C}_{33}$ without the thermal and piezoelectric couplings is calculated and is shown in Fig. 2 as $\overline{C}_{33}^E$. It is immediately seen that the coupling is not the major cause of the minimum of $\overline{C}_{33}$. Further investigate into this is presented in the Appendix. Based on the examination in the Appendix, we can make a somewhat restrictive conclusion
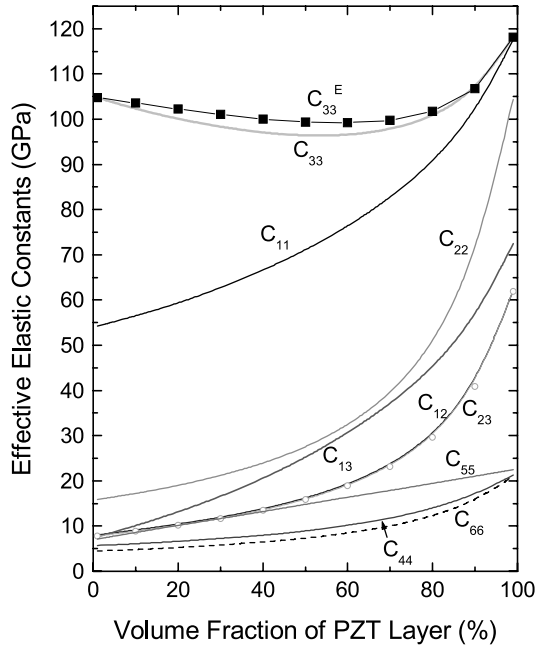
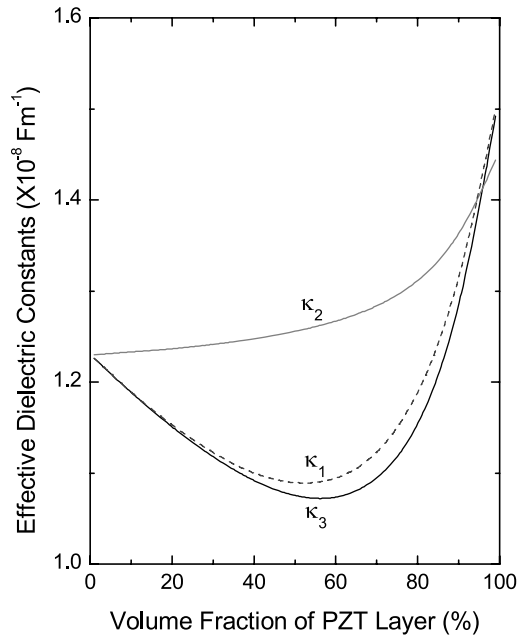**Figure 2.** Change of effective elastic constants for varying volume ratio (graphite/epoxy-PZT composite).



**Figure 3.** Change of effective dielectric constants for varying volume ratio (graphite/epoxy-PZT composite).
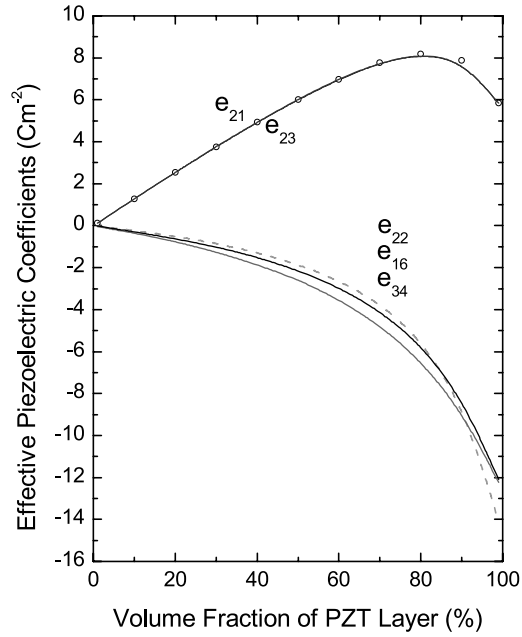
**Figure 4.** Change of effective piezoelectric coefficients for varying volume ratio (graphite/epoxy-PZT composite).
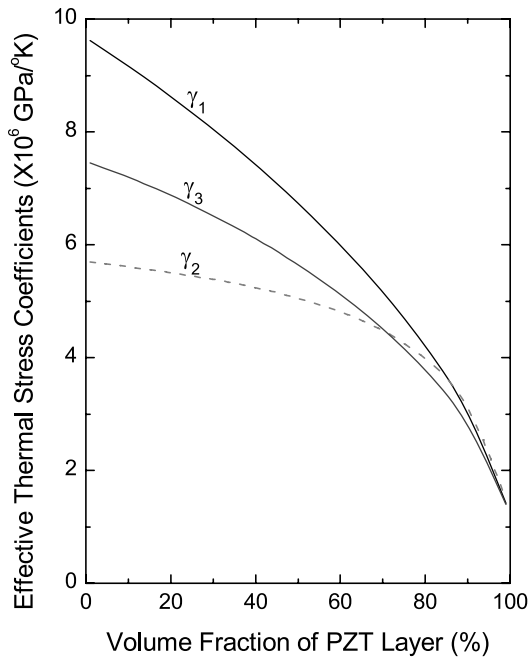


**Figure 5.** Change of effective thermal stress coefficients for varying volume ratio (graphite/ epoxy-PZT composite).
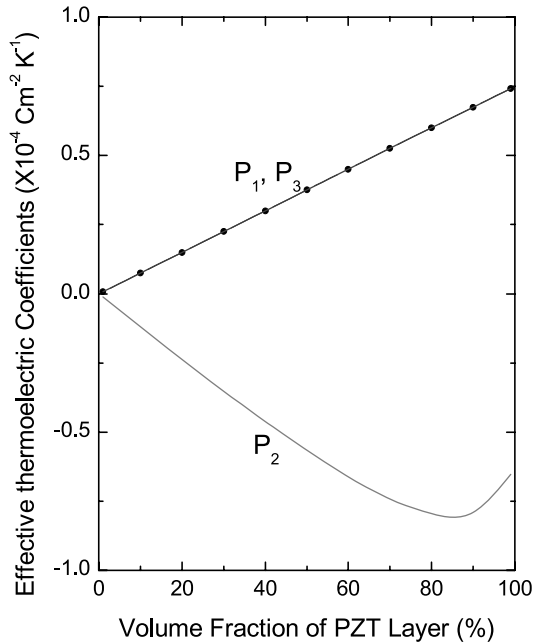
**Figure 6.** Change of effective thermoelectric coefficients for varying volume ratio (graphite/epoxy-PZT composite).

that effective properties of a multilayered composite can have an extremum at an intermediate volume fraction.

### 3.3. Piezoelectric–Piezomagnetic Composite

Numerical calculations are also performed for a layered $BaTiO_3$–$CoFe_2O_4$ composite. $BaTiO_3$ is the transversely isotropic piezoelectric material and $CoFe_2O_4$ is the transversely isotropic piezomagnetic material. The effective material properties are calculated for varying $BaTiO_3$ volume fraction. The constituent material constants are shown in Table 1.

From all effective constants that were calculated, only the effective nonzero piezomagnetic and magnetoelectric ($\bar{\zeta}_{33}$) coefficients (the coupled effects) are shown in Figs 7 and 8 to avoid repetition. Although both $BaTiO_3$ and $CoFe_2O_4$ do not have the magnetoelectric effect on their own as shown in Table 1, the multilayered composite exhibits a very strong magnetoelectric effect, which will be very useful in many applications. Similar results have been found in other composite configurations (fibrous and particulate) made of the same constituents [12, 13]. The effective magnetoelectric coefficient has a maximum value at the volume fraction around 42%. The magnetoelectric coefficients of other types of composite fabricated with $BaTiO_3$ fibers [12] and ellipsoidal particles [13] in $CoFe_2O_4$ matrix are shown together in Fig. 8. It is interesting that the magnetoelectric coefficient increases according as the inclusion phase ($BaTiO_3$) becomes more continuous,
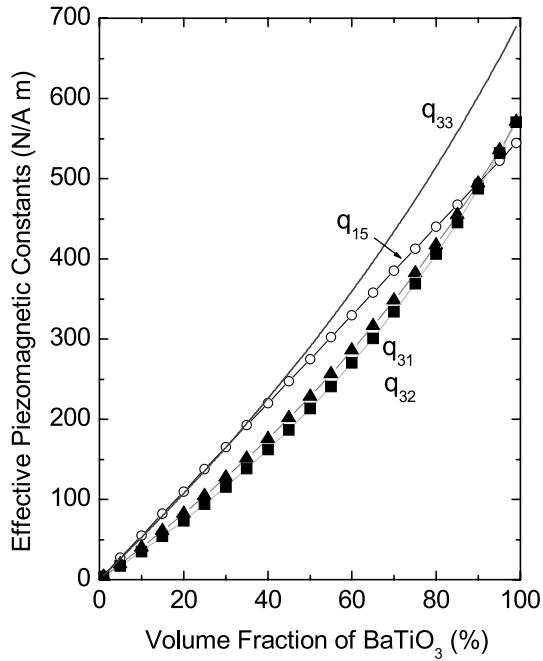
**Figure 7.** Change of effective piezomagnetic constants for varying volume ratio ($BaTiO_3$–$CoFe_2O_4$ composite).
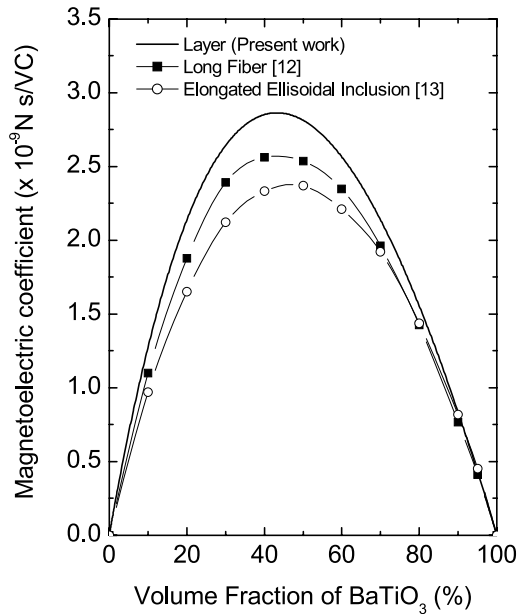


**Figure 8.** Change of magnetoelectric coefficient for varying volume ratio ($BaTiO_3$–$CoFe_2O_4$ composite).

which seems to be physically reasonable and validates the proposed method and the calculated results.

The magnetoelectric coefficient of the $BaTiO_3$–$CoFe_2O_4$ composite can be derived in an explicit form from (31), (33) and (34):

$$\bar{\zeta}_{33} = \nu_1 \nu_2 e_{34}^{(1)} q_{34}^{(2)} / \left(\nu_1 C_{44}^{(1)} + \nu_2 C_{44}^{(2)}\right), \tag{35}$$

where 1 and 2 denote $BaTiO_3$ and $CoFe_2O_4$ phases, respectively. It can be easily shown that $\bar{\zeta}_{33}$ has a maximum value between $0 < \nu_1 < 1$ if $e_{34}^{(1)} q_{34}^{(2)} > 0$, $C_{44}^{(1)} > 0$, $C_{44}^{(2)} > 0$, and $\nu_1 \nu_2 e_{34}^{(1)} q_{34}^{(2)} \gg (\nu_1 C_{44}^{(1)} + \nu_2 C_{44}^{(2)})$. The specific location of the maximum will depend on the material constants $(e_{34}^{(1)}, q_{34}^{(2)}, C_{44}^{(1)}, C_{44}^{(2)})$ in (35).

Recently, the $BaTiO_3$–$CoFe_2O_4$ composite has been fabricated in the form of a nano film [14], demonstrating the material's great potential for numerous applications in nanoscale multifunctional devices.

## 4. Summary

By extending our previous work on purely elastic multilayers [6], a unified method is developed for evaluating the effective material properties of generally anisotropic multilayered media whose constituents exhibit thermoelastic, piezoelectric, piezomagnetic effects and coupled effects between these. Examples of applications are given for the effective properties of the piezoelectric–piezomagnetic $BaTiO_3$–$CoFe_2O_4$ composite and the piezo-thermoelastic PZT-graphite/epoxy composite. The $BaTiO_3$–$CoFe_2O_4$ composite exhibits a remarkably strong magnetoelectric effect that does not exist in its constituents. It is shown that the magnetoelectric effect in the multiplayer composite is higher than those in matrix-inclusion type composites. It is shown that some of the effective properties of a multilayer composite can have an extremum at an intermediate volume fraction. The present method is essentially valid when the material properties are constant in every layer. However, the method can be readily applied to a layered composite with continuously varying material properties (graded composite) by dividing the layers into a sufficiently large number of sublayers.

## References

1. I. Alshits, A. N. Darinskii and J. Lothe, On the existence of surface waves in half-anisotropic elastic media with piezoelectric and piezoelectric properties, *Wave Motion* **16**, 265–283 (1992).

2. J. Ryu, A. V. Carazo, K. Uchino and H. E. Kim, Magnetoelectric properties in piezoelectric and magnetostrictive laminate composites, *Japan J. Appl. Phys.* **40**, 4948–4951 (2001).

3. A. N. Norris, The effective moduli of layered media — a new look at an old problem, in: *Micromechanics and Inhomogeneity: the Toshio Mura 65th Anniversary Volume*, G. J. Weng, M. Taya and H. Abe (Eds), pp. 321–339. Springer-Verlag, New York, USA (1990).

4. P. C. Chou, J. Carleone and C. M. Hsu, Elastic constants of layered media, *J. Compos. Mater.* **6**, 80–93 (1972).

5. N. J. Pagano, Exact moduli of anisotropic laminates, in: *Mechanics of Composite Materials*, G. P. Sendeckyj (Ed.), Vol. 2, pp. 23–45. Academic Press, New York, USA (1974).
6. J.-Y. Kim, Effective elastic constants of anisotropic multilayers, *Mech. Res. Commun.* **28**, 97–101 (2000).
7. E. Akcakaya and G. W. Farnell, Effective elastic and piezoelectric constants of superlattices, *J. Appl. Phys.* **64**, 4469–4473 (1988).
8. Z. Chen, S. Yu, L. Meng and Y. Lin, Effective properties of layered magneto-electro-elastic composites, *Compos. Struct.* **57**, 177–182 (2002).
9. M. Paley and J. Aboudi, Micromechanical analysis of composites by the generalized cells model, *Mech. Mater.* **14**, 127–139 (1992).
10. L. Wang and S. I. Rokhlin, Floquet wave homogenization of periodic anisotropic media, *J. Acoust. Soc. Amer.* **112**, 38–45 (2002).
11. V. M. Levin and A. G. Luchaninov, On the effective properties of thermo-piezoelectric matrix composites, *J. Phys. D: Appl. Phys.* **34**, 3058–3063 (2001).
12. C.-W. Nan, Magnetoeletric effect in composites of piezoelectric and piezomagnetic phases, *Phys. Rev. B* **50**, 6082–6088 (1994).
13. J. H. Huang and W.-S. Kuo, The analysis of piezoelectric/piezomagnetic composite materials containing inclusions, *J. Appl. Phys.* **81**, 1378–1386 (1997).
14. C.-W. Nan, G. Liu, Y. Lin and H. Chen, Magnetic field induced electric polarization in multiferroic nanostructures, *Phys. Rev. Lett.* **94**, 197203 (2005).

## Appendix: The Minimum of $\overline{C}_{33}^E$

Here we investigate if an effective elastic constant of multilayer composites can have an extremum at a volume fraction other than 0 and 1. To simplify the algebra, let us consider a purely elastic multilayer composite with two sublayers that have the orthotropic symmetry. The expression of $\overline{C}_{33}^E$ derived from (31), (33) and (34) ignoring the thermal and piezoelectric effects is

$$\overline{C}_{33}^E = v_1 C_{33}^{(1)} + v_2 C_{33}^{(2)} + F, \tag{A.1}$$

$$
F = -\left( v_1 \frac{C_{23}^{(1)2}}{C_{22}^{(1)}} + v_2 \frac{C_{23}^{(2)2}}{C_{22}^{(2)}} \right) + \left( v_1 \frac{C_{23}^{(1)}}{C_{22}^{(1)}} + v_2 \frac{C_{23}^{(2)}}{C_{22}^{(2)}} \right)
$$
$$
\times \frac{v_1 C_{23}^{(1)} C_{22}^{(2)} + v_2 C_{23}^{(2)} C_{22}^{(1)}}{v_1 C_{22}^{(2)} + v_2 C_{22}^{(1)}}. \tag{A.2}
$$

Since the first term in (A.1) is a linear function that does not have an extremum, the second term is examined. Consider a special case $C_{22}^{(1)} \approx C_{22}^{(2)}$, then it can be shown that the second term is reduced:

$$
F = -\frac{C_{23}^{(1)2}}{C_{22}^{(1)}} v_1 (1 - v_1) \left( \frac{C_{23}^{(2)}}{C_{23}^{(1)}} - 1 \right)^2. \tag{A.3}
$$

This function vanishes at $v_1 = 0$ and $v_1 = 1$ and has a minimum in $0 < v_1 < 1$ with its magnitude determined by the elastic constants in (A.3). This proves that at least in this special case the $\overline{C}_{33}^E$ can have a minimum in $0 < v_1 < 1$ as shown in Fig. 2.